J MATER RES TECHNOL. 2018;xxx(xx):xxx–xxx

Available online at www.sciencedirect.com

jmr&t Journal of Materials Research and Technology

www.jmrt.com.br

Original Article

Lanthanum titanate nanometric powder potentially for rechargeable Ni-batteries: Synthesis and electrochemical hydrogen storage

J. Henao[a,*], Y. Pacheco[b], O. Sotelo[b], M. Casales[b], L. Martinez-Gómez[b]

[a] CONACyT-CIATEQ A.C., Parque Industrial Bernardo Quintana, Av. Manantiales 23-A, El Marqués, Querétaro C.P.76246, Mexico

[b] Instituto de Ciencias Físicas, Universidad Nacional Autónoma de México (UNAM), Avenida Universidad s/n, 62210 Cuernavaca, Morelos, Mexico

ARTICLE INFO

Article history:
Received 14 October 2017
Accepted 15 May 2018
Available online xxx

Keywords:
Rare-earths
Ni batteries
Perovskites
Hydrogen absorption

ABSTRACT

$La_2Ti_2O_7$ nanosized powder was prepared and evaluated as novel negative electrode material for Ni/oxide rechargeable batteries. $La_2Ti_2O_7$ nanosized powder was synthesized at 850 °C within 5 h by the well-known citric-acid sol–gel route. The synthetized powder had an irregular morphology with a particle size below 100 nm and a tendency to form clusters. $La_2Ti_2O_7$ had a perovskite-type layered structure and presented a maximum electrochemical hydrogen uptake capacity of 224 mA h/g corresponding to 0.84 wt.% of hydrogen. Electrochemical studies revealed that the $La_2Ti_2O_7$ compound can be considered an alternative electrode material for Ni/oxide rechargeable batteries since it exhibits a good cycling stability after activation.

1. Introduction

The demand for reliable and efficient battery technology has led to increased interest in the development of new type of materials. Particularly, efforts have been made to determine new materials for nickel battery technology that can provide hydrogen storage under different operational conditions. These materials include intermetallic alloys, amorphous alloys, perovskite-type oxides, and carbon materials [1–4]. Metallic alloys (intermetallic and amorphous) are usually used as negative electrode materials in the well-known nickel metal hydride (Ni/MH) battery technology [1]. Alternatively, metal oxides and perovskite-type oxides have become a prominent option to replace conventional metallic alloys in Ni/oxide rechargeable battery technology [2,5]. Oxide compounds present advantageous properties over metallic materials since they are able to operate in strong basic environments and at high temperatures without losing their electrochemical performance. In recent years, a large amount of development has focused on Ni/oxide batteries using perovskite-type oxides with the general formula ABO_3 [2]. Hydrogen uptake

* Corresponding author.
E-mail: jhenao@conacyt.mx (J. Henao).

https://doi.org/10.1016/j.jmrt.2018.05.019

Please cite this article in press as: Henao J, et al. Lanthanum titanate nanometric powder potentially for rechargeable Ni-batteries: Synthesis and electrochemical hydrogen storage. J Mater Res Technol. 2018. https://doi.org/10.1016/j.jmrt.2018.05.019

in perovskite-type materials is possible due to the insertion of hydrogen protons into the oxygen-related positions within the crystalline structure of perovskites. Some examples are the doped $La_{0.8}Sr_{0.2}FeO_3$ and $La_{0.6}Sr_{0.4}Co_{0.2}Fe_{0.8}O_3$ compositions with an electrochemical capacity of 50 and 51 mA h/g at room temperature, respectively [5,6].

Previous studies focused on improving the electrochemical properties of ABO_3 perovskite electrodes have reported that nanometric powders present better hydrogen absorption properties than micrometric ones since the electrolyte–electrode contact area is increased, leading to enhanced efficiency of the electrochemical reaction [7]. One example of this finding is the nanometric $LaFeO_3$ perovskite-type powder that presented an electrochemical capacity of 130 mA h/g at room temperature; this result was remarkably higher than the 80 mA h/g achieved from similar micrometric powder [7,8].

Alternatively, lanthanide titanium oxides with the general formula $RE_2Ti_2O_7$ (RE = rare earth) have received a large amount of attention in the past years because these oxides present interesting physical properties, including ferroelectric, optical, and photocatalytic properties [9,10]. Although the formula $A_2B_2O_7$ is usually associated with the pyrochlore structure [11], lanthanide titanium oxides belong to the perovskite-layered structure family (for A = La to Nd) which possesses narrow depletion layers and high quantum yields and therefore provides strong photocatalytic activity and high thermal stability [12]. To the best of our knowledge, most of the perovskite-type lanthanide titanium oxides, especially the $La_2Ti_2O_7$ oxide, have been involved in applications related to dielectric and ferroelectric properties (photocatalysis), but no papers have investigated its hydrogen storage property.

In the present study, the suitability of using $La_2Ti_2O_7$ perovskite-type nanometric powder as a novel negative electrode material for Ni/oxide batteries has been prioritized. Herein, the citric acid sol–gel (CASG) route has been used to obtain $La_2Ti_2O_7$ nanometric powder. The CASG route is advantageous over the conventional synthesis route since it is a low-temperature synthesis method that produces homogeneous powders. The synthetized powder was used to prepare cold-pressed electrodes that were then evaluated via electrochemical measurements.

2. Experimental

2.1. Synthesis of $La_2Ti_2O_7$ nanometric powder and preparation of electrodes

Tetrabutyl titanate ($Ti(OBu)_4$) (Aldrich) and La_2O_3 (99.9% purity, Aldrich) were used as the precursors of Ti and La in the CASG synthesis route. The molar ratio of La/Ti was fixed at 1/1. La_2O_3 powder (0.005 mol) was dispersed in a spot of water, and then 5 mL of concentrated HNO_3 was added to it in droplets to dissolve the oxide. Subsequently, citric acid (0.04 mol) was dissolved in 5 mL of H_2O and then poured into the solution. The mixture was thoroughly stirred by the magnetic mixer. At this point, $Ti(OBu)_4$ (0.01 mol) was added with vigorous stirring and in a 60 °C liquid bath. After 0.5 h, a homogeneous transparent solution was formed. The solution was heated at 120 °C to vaporize the water. Four hours later, the mixture solution changed from a colorless solution to a white gel. Then, the gel was taken out and calcined in a Thermo Scientific Thermolyne furnace (F30428C-80 XL) at 850 °C for 5 h in air. The preheating ramp used was 7 °C/min for about 2 h up to 850 °C. After the calcination, the samples were cooled to room temperature within the furnace for 12 h at a cooling rate of 1.1 °C/min.

The $La_2Ti_2O_7$ electrodes were prepared using the so-called "latex" method. The $La_2Ti_2O_7$ nanometric powder was mixed with black carbon to ensure good conductivity and polytetrafluoroethylene (PTFE) to provide the compound with more elasticity. The weight ratio of the mixture was 90:5:5 for $La_2Ti_2O_7$, carbon black, and PTFE, respectively. Ethyleneglycol was added to the mixture in order to form a viscoelastic paste. The paste was deposited onto a 1 cm^2 Ni-mesh and then this was dried for 2 h to evaporate the solvent. The electrodes were finally obtained by cold-pressing the deposited mixture onto the Ni-mesh at a pressure of 40 MPa.

2.2. Physical and electrochemical measurements

Differential and thermogravimetric curves (DSC–TGA) were evaluated on a simultaneous thermal analysis instrument (DSC-TGA-SDT Q600, TA Instruments) from room temperature up to 900 °C and at a heating rate of 10 °C/min. X-ray diffraction (XRD) measurements were conducted using a specular reflection mode (Bruker D8 Advanced, Cu Ka radiation, $k = 0.154056$ nm) over the angular range of $20° < \Theta < 80°$ with a step size of 0.008° and a measuring time of 300 s per step. The particle size distribution of the $La_2Ti_2O_7$ powder was determined using a laser diffraction equipment (LS1057083 Laser Diffraction, Malvern Instruments). The morphology of the product was determined by scanning electron microscopy (SEM, JEOL 7600). The electrochemical performance of the prepared lanthanum titanate oxide was tested in a conventional three-electrode open-air-cell (Potentiostat-Galvanostat, Gamry 1000E) using $La_2Ti_2O_7$ as the working electrode, Hg/HgO as the reference electrode, $Ni(OH)_2$ as the counter-electrode, and KOH (6 M) solution as the electrolyte. The charge–discharge properties of the negative electrode were investigated using the chronopotentiometry technique. The working electrodes were fully charged and discharged at constant current densities of 10, 30, 60, and 125 mA/g. The charge–discharge properties of the negative electrode were also investigated using cyclic voltammetry experiments and a chronoamperometry technique. Cyclic voltammograms were recorded between −0.4 and −1.3 V compared with the Hg/HgO reference electrode at a scan rate of 1 mV/s. A chronoamperometry technique was applied to estimate the hydrogen diffusion coefficient at different states of charge, after activation. Linear polarization scans were also recorded at the rate of 0.1 mV/s from −5 to +5 mV with respect to the open circuit potential.

Please cite this article in press as: Henao J, et al. Lanthanum titanate nanometric powder potentially for rechargeable Ni-batteries: Synthesis and electrochemical hydrogen storage. J Mater Res Technol. 2018. https://doi.org/10.1016/j.jmrt.2018.05.019

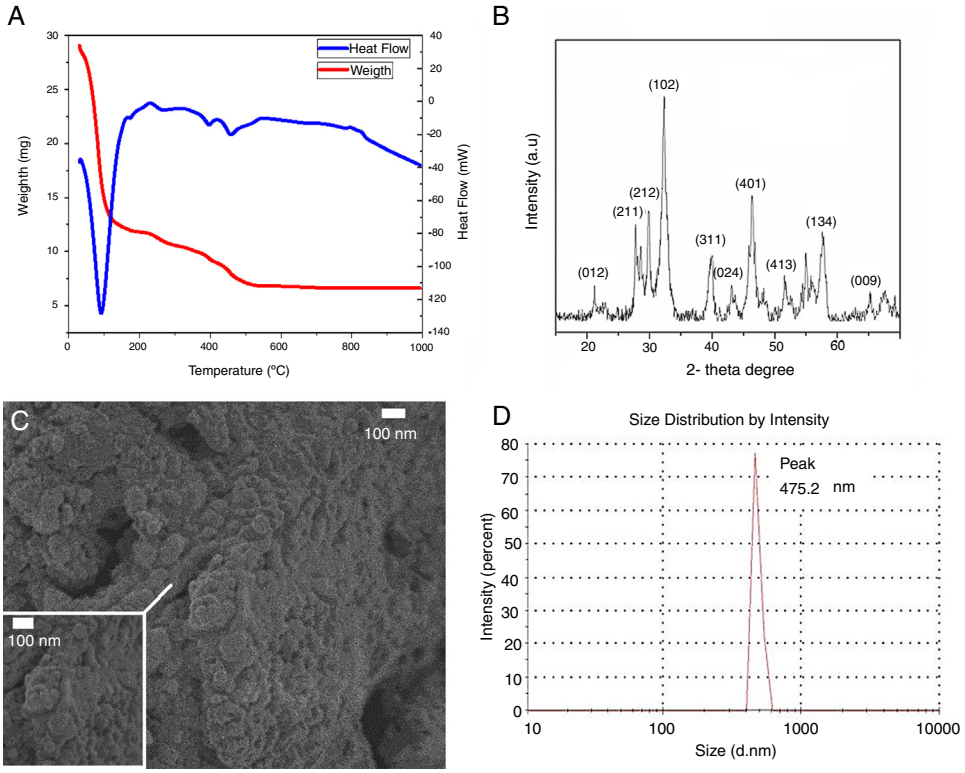

Figure 1 – Characterization results: (a) DSC–TGA curve of the $La_2Ti_2O_7$ precursor gel; (b) XRD pattern of the $La_2Ti_2O_7$ powder; (c) SEM micrograph of the powder obtained; (d) LS analysis.

3. Results and discussion

3.1. *Characterization of the synthetized powder*

TGA–DSC measurements were carried out on the precursor gel to reveal the synthesis temperature corresponding to the $La_2Ti_2O_7$ oxide obtained by the CASG route. Fig. 1a shows the TGA–DSC curves of the $La_2Ti_2O_7$ precursor gel. The DSC curve has four peaks. The first endothermic peak (91 °C) with relatively large weight loss (60%) is caused by the decomposition of the aqueous products [13,14]. The second endothermic peak (230 °C) is attributed to the evaporation and burning of the organic substance. A third exothermic peak (395 °C) is also observed and is caused by the combustion of the remaining organic substance, while the fourth exothermic peak (457 °C) is related to the crystal lattice energy released during the formation of the perovskite-type structure. The last exothermic peak is associated with the final formation of the $La_2Ti_2O_7$ compound. The measured overall weight loss was 77.26% and indicates the complete removal of all of the citric acid and all of the organic substance. No further weight loss was found from 600 up to 1000 °C, suggesting that the $La_2Ti_2O_7$ compound can be successfully fabricated in this temperature range. Consequently, the temperature selected to prepare $La_2Ti_2O_7$ was 850 °C to ensure complete transformation. Fig. 1b displays the XRD pattern of the prepared powder at 850 °C (2 h), which is quite consistent with a single perovskite-type layered phase of $La_2Ti_2O_7$. The XRD pattern is indexed based on a monoclinic lattice ($a = 7.8262$ Å, $b = 12.8914$ Å, $c = 5.49$ Å, and $\beta = 98.081°$) (JCPDS 81-1066). Fig. 1c and d shows the SEM and LS results of $La_2Ti_2O_7$ prepared by CASG, respectively. The obtained powder presents an irregular morphology typical of chemical methods; it also displays a nanometric particle size (<100 nm) with a tendency for agglomeration. The LS results prove that $La_2Ti_2O_7$ particles agglomerate into clusters of about 475 nm. Overall, the present results show that it is feasible to produce $La_2Ti_2O_7$ nanopowders using CASG. This powder is usually fabricated by a conventional solid-state method at a high temperature (1100 °C) and long calcination time (50 h) [15]; however, the CASG results are advantageous because the $La_2Ti_2O_7$ powder can be successfully prepared at a relatively low temperature (850 °C) and a shortened calcination time (5 h). The solid-state reaction is a two-step process involving a mechanical mixture of the precursors followed by heat treatment. To induce the mobility of the atoms to form the perovskite-type compound, calcination times are often long, between 12 and 50 h, and at temperatures ranging from 1100 to 1400 °C [16,17]. Thus, the prolonged times and high temperatures involved in the solid-state method represent higher energy consumption in comparison to the CASG route, which involves shorter times and lower calcination temperatures.

3.2. *Electrochemical performance*

Cyclic voltammetry experiments were carried out to reveal the electrochemical reduction–oxidation reactions of the $La_2Ti_2O_7$ electrode in 6 M KOH aqueous solution. Fig. 2 shows the cyclic voltammogram of the $La_2Ti_2O_7$ negative electrode. A

Please cite this article in press as: Henao J, et al. Lanthanum titanate nanometric powder potentially for rechargeable Ni-batteries: Synthesis and electrochemical hydrogen storage. J Mater Res Technol. 2018. https://doi.org/10.1016/j.jmrt.2018.05.019

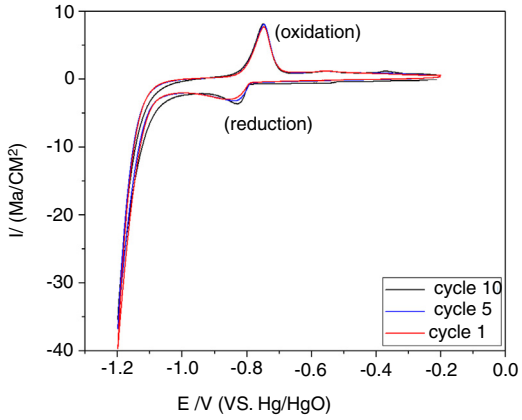

Figure 2 – Cyclic voltammogram of the $La_2Ti_2O_7$ electrode.

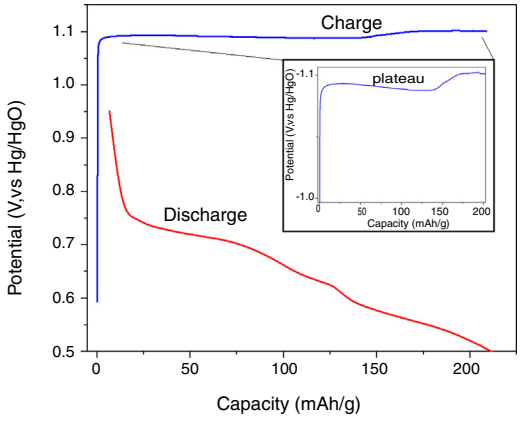

Figure 3 – Charge–discharge curve of the $La_2Ti_2O_7$ electrode.

remarkable oxidation peak appears at −0.75 V with respect to the Hg/HgO reference electrode, and a strong reduction peak appears at −0.825 V with respect to the Hg/HgO reference electrode. This pair of redox peaks suggests that a reversible electrochemical reaction is occurring on the $La_2Ti_2O_7$ working electrode. Interestingly, these peaks exhibit similar potential values compared with metal hydride electrodes [18]. The desorption peak of hydrogen appears prior to the electrochemical oxidation peak of hydrogen, suggesting the possible existence of strong hydrogen chemisorption. Moreover, the reduction peak becomes more defined with increasing number of cycles, indicating that the $La_2Ti_2O_7$ electrode, unlike most ABO_3-pervoskite-type oxides reported up to date [2], must be activated before reaching its maximum capacity (see also Fig. 4).

Fig. 3 displays the typical charge–discharge curves for the $La_2Ti_2O_7$ electrode. Interestingly, the charge–discharge curves of the cell are comparable to those of conventional hydrogen storage alloys [19] and those of conventional ABO_3-pervoskite oxides [2,20], presenting an electrochemical discharge capacity of about 224 mA h/g. The charge curve shows a long and flat potential plateau, possibly due to the formation of stable chemical bonds between hydrogen atoms and oxygen in the oxide structure (see inset in Fig. 3). Interestingly, the discharge

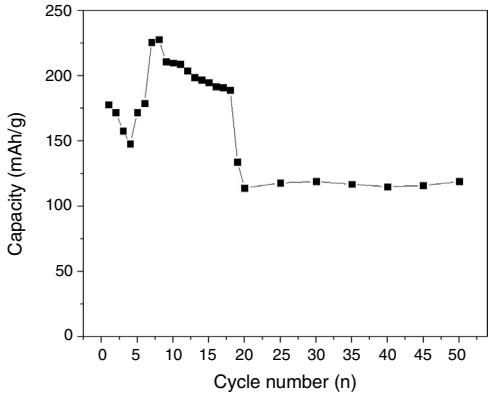

Figure 4 – Cycling performance of the $La_2Ti_2O_7$ electrode.

potential plateau of the $La_2Ti_2O_7$ electrode starts at approximately −0.75 V, which is significantly lower than the potential plateau values in conventional ABO_3-perovskite electrodes (~−1.2 V) [2]. This difference between ABO_3 and $A_2B_2O_7$ perovskite structures could be caused by the presence of storing sites in the $La_2Ti_2O_7$ structure with stronger repulsive forces from the local environment, resulting in an increase in site energy and, therefore, in a lower potential compared with ABO_3 electrodes [21].

Fig. 4 shows the cycling performance of the $La_2Ti_2O_7$ electrode at a constant current density of 30 mA h/g at room temperature. This test is usually performed to reveal the stability of electrode materials as a function of cycle number. The initial electrochemical discharge capacity of the $La_2Ti_2O_7$ electrodes was 178 mA h/g, corresponding to ~0.66 wt.% hydrogen. During the fourth to seventh cycle, the discharge capacities increased up to a maximum value of 224 mA h/g at the eighth cycle. This result reflects the electrochemical activation process of $La_2Ti_2O_7$ that is necessary to achieve the intrinsic hydrogen storage capabilities of the electrode. From the eighth cycle to the 20th cycle, the reversible capacity was kept around 200 mA h/g; however, after the 20th cycle, an important capacity decay occurs, corresponding to a 47% decay (53% capacity retention). Despite the significant drop in the discharge capacity after the 20th cycle, the electrochemical capacity stabilized at approximately 114 mA h/g for more than 20 charge–discharge cycles up to the end of the test (50th cycle). This long, stable capacity values as a function of cycle number is common in perovskite-type materials [2].

To compare the electrode performance at different discharge currents, the high rate dischargeability (HRD) was evaluated. HRD is a parameter that reflects the discharge capability at different discharge current densities and can be dominated by the charge transfer rate at the electrode surface and the diffusion rate of hydrogen atoms in the bulk of the electrode [22]. HRD can be calculated by the following equation [23]:

$$\mathrm{HRD} = \frac{C_n}{C_{\max}} * 100\% \quad (1)$$

Herein, C_n is the discharge capacity at a discharge current density of n mA/g and C_{max} is the discharge capacity

Please cite this article in press as: Henao J, et al. Lanthanum titanate nanometric powder potentially for rechargeable Ni-batteries: Synthesis and electrochemical hydrogen storage. J Mater Res Technol. 2018. https://doi.org/10.1016/j.jmrt.2018.05.019

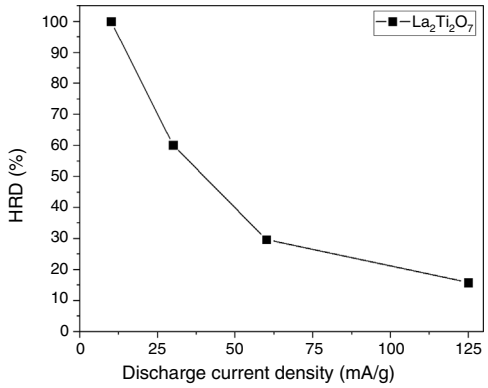

Figure 5 – High rate dischargeability of the $La_2Ti_2O_7$ electrode as a function of the discharge current density.

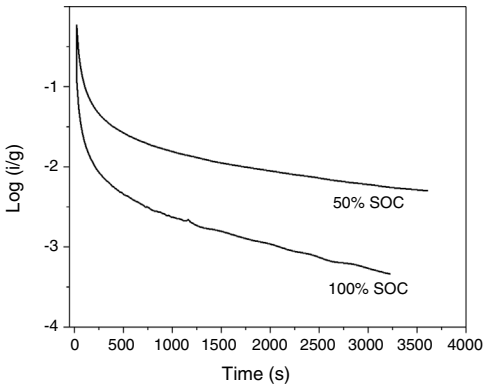

Figure 6 – Chronoamperometric semi-logarithm curve of the $La_2Ti_2O_7$ electrode.

at the current density of 125 mA/g. The experimental HRD curve is shown in Fig. 5. According to these results, the performance of the $La_2Ti_2O_7$ electrode depends on the discharge rate, experiencing a progressive reduction in its electrochemical capacity when the discharge current density increases. The $La_2Ti_2O_7$ electrode presents an electrochemical capacity of 379 mA h/g at a current density of 10 mA/g; nevertheless, its discharge ability is reduced only to 60.23 mA h/g at 125 mA/g (HRD ~ 16%). This behavior was also seen in hydrogen storage alloys and in perovskites in previous studies [22,24] and has been ascribed to the increase of electrochemical reaction kinetics on the electrode surface when the discharge rate increases. In terms of discharge capacity, the $La_2Ti_2O_7$ electrode presents values that are close to those capacity values in ABO_3-perovskite oxides. For instance, $LaFeO_3$, $La_{0.6}Sr_{0.4}FeO_3$, and $La_{0.6}Sr_{0.4}Co_{0.2}Fe_{0.8}O_3$ have capacity values between 50 and 80 mA h/g at a current density of 125 mA h/g and at room temperature [2,5].

The hydrogen diffusion coefficient of the $La_2Ti_2O_7$ oxide was also estimated in the present study by the potential-step discharge technique. This method consists of applying a potential step while monitoring the anodic current–time response. The semi-logarithmic curve obtained from this experiment can be divided into two-time regions [25]. In the first-time region, the current experiences a rapid decrease due to the fast consumption of hydrogen on the surface of the electrode. This region is strongly governed by the charge transfer kinetics and/or by charge transfer and diffusion (mixed kinetics). However, in the second-time region, the current gradually decreases in a linear manner with time and is controlled by the hydrogen diffusion. Fig. 6 shows the semi-logarithmic curve of the anodic current–time response for the $La_2Ti_2O_7$ electrode at 50 and 100% SOC. As expected, the current–time response of the $La_2Ti_2O_7$ electrode presents both regions (mixed and diffusion controlled), which are decaled to each other due to the effect of SOC. According to the model proposed by Zheng et al. [26], the hydrogen diffusion coefficient D_H can be estimated from the diffusion-controlled region in the electrode bulk by the following equation:

$$\log i = \log\left[\frac{6FD_H}{da^2}(C_0 - C_s)\right] - \frac{\pi^2}{2.303}\frac{D_H t}{a^2} \quad (2)$$

where i is the anodic current density (A/g), D_H is hydrogen diffusion coefficient (cm^2/s), d is density of the compound (g/cm^3), a is the average radius of the particles, C_0 is the initial hydrogen concentration in the bulk of the electrode (mol/cm^3), C_s is the surface hydrogen concentration of the electrode (mol/cm^3), and t is the discharge time (s). According to Eq. (2), D_H was estimated as 3.87×10^{-14} and 1.51×10^{-13} for the $La_2Ti_2O_7$ electrode at 50 and 100% SOC, respectively, that is, D_H decreases with the state of charge. These results can be ascribed to the fact that diffusion paths are associated with oxygen-related positions within the perovskite-oxide structure. When the electrode begins the charge process, many of these oxygen positions become occupied by hydrogen in a well-established O–H chemical bond. However, when the number of H^+ ions inserted into the unit cell of perovskite oxides increases, the O–H bond reduces its strength and consequently the activation energy necessary to break the O–H bond, facilitating hydrogen ion transportation [27]. Interestingly, the $La_2Ti_2O_7$ electrode presents similar D_H values compared with other perovskite-type oxide electrodes and has lower D_H values than intermetallic compounds ($<D_H \sim 10^{-10}$ cm^2/s), which is due to the nature of the ion insertion and transport in perovskites with respect to intermetallic alloys [2,5,27].

In order to reveal more information about the kinetics of the process, linear polarization curves were obtained. Fig. 7 shows the linear polarization curve of the $La_2Ti_2O_7$ electrode. Fig. 7 shows that the polarizing current has a linear relationship with overpotential in the overpotential range from −5 to 5 mV. The linear polarization technique involves the hydrogen reduction–oxidation reactions on the surface layer of the oxide electrode and, as a result, the charge transfer rate at the electrode surface can be evaluated by the exchange current density (I_0) according to the following equation [28]:

$$I_0 = \frac{RT}{FR_p} \quad (3)$$

where R is the gas constant ($R = 8.314\,J\,mol^{-1}\,K^{-1}$), T is the absolute temperature (K), F is the Faraday constant ($F = 96\,485\,C\,mol^{-1}$), and R_p is the polarization resistance (mΩ) (i.e., the reciprocal of the slope in Fig. 7). According to Eq. (3), the exchange current density of the $La_2Ti_2O_7$ electrode

Please cite this article in press as: Henao J, et al. Lanthanum titanate nanometric powder potentially for rechargeable Ni-batteries: Synthesis and electrochemical hydrogen storage. J Mater Res Technol. 2018. https://doi.org/10.1016/j.jmrt.2018.05.019

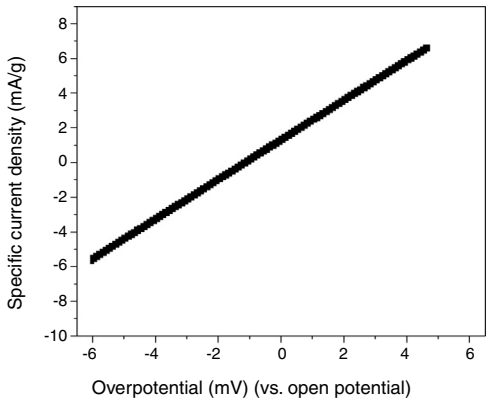

Figure 7 – Linear polarization curve of the $La_2Ti_2O_7$ electrode.

is 27.8 mA/g. This value has the same order of magnitude as the exchange current density values reported for perovskite-oxides in previous reports [2]. For instance, the nano-$LaFeO_3$ perovskite-type electrode has a I_0 value of 28 mA/g and a hydrogen diffusion coefficient on the order of 10^{-14} at room temperature [7]. These results suggest that the kinetics and transport properties of the $La_2Ti_2O_7$ electrode are both quite similar to those reported for ABO_3-perovskite oxides.

4. Conclusions

Nanometric $La_2Ti_2O_7$ powder was prepared by means of the citric acid sol–gel route, which is currently a suitable technique to reduce energy consumption with respect to the conventional solid-state synthesis route. The as-prepared nanometric $La_2Ti_2O_7$ powder presented hydrogen-storage properties in alkaline solution at room temperature. $La_2Ti_2O_7$ had promising hydrogen-absorption capabilities with a total maximum discharge capacity of 224 mA h/g and only 47% capacity decay, corresponding to 114 mA h/g, after 50 cycles at room temperature. These results are notably better than the hydrogen-storage properties of some ABO_3-perovskite oxides at room temperature. Thus, $La_2Ti_2O_7$ can be regarded as a potential candidate for negative electrode material that can be used with rechargeable Ni/oxide batteries. The present study represents a first approach for developing $A_2B_2O_7$-perovskite-layered oxides as negative electrode material for Ni/oxide batteries. Therefore, further studies are encouraged to further analyze the hydrogen-absorption mechanisms as well as application differences with respect to conventional ABO_3-perovskite oxides.

Author contribution statement

All the authors have made a significant contribution to this manuscript.

Conflicts of interest

The authors declare no conflict of interests regarding the publication of this manuscript.

Acknowledgements

This work was supported by the National Science and Technology Council and the Secretary of Energy of Mexico "CONACYT-SENER-Sustentabilidad Energética" (Project No. 232611). Eng. Y. Pacheco would like to thank the support of the National Science and Technology Council (CONACYT) (grant No. 445176).

REFERENCES

[1] Tliha M, Khaldi C, Boussami S, Fenineche N, El-Kedim O, Mathlouthi H, Lamloumi J. Kinetic and thermodynamic studies of hydrogen storage alloys as negative electrode materials for Ni/MH batteries: a review. J. Solid State Electrochem 2014;18(3):577–93.
[2] Henao J, Martinez-Gomez L. On rare-earth perovskite-type negative electrodes in nickel–hydride (Ni/H) secondary batteries. M. Renew. Sustain. Ener 2017; 6(2):7.
[3] Bagheri N, Aghaei A, Vlachopoulos N, Skunik-Nuckowska M, Kulesza P, Häggman L, Hagfeldt A. Physicochemical identity and charge storage properties of battery-type nickel oxide material and its composites with activated carbon. Electrochim. Acta 2016;194:480–8.
[4] Zhang YH, Yuan ZM, Yang T, Hou ZH, Zhao DL. Properties of mechanically milled nanocrystalline and amorphous Mg–Y–Ni electrode alloys for Ni–MH batteries. Acta Metall. Sin. Engl 2015;28(7):826–36.
[5] Henao J, Sotelo O, Casales M, Martinez-Gomez L. Electrochemical performance of the rare-earth perovskite-type oxide $La_{0.6}Sr_{0.4}Co_{0.2}Fe_{0.8}O_3$ as negative electrode material for Ni/oxide rechargeable batteries. M. Renew. Sustain. Ener 2017;6(16).
[6] Deng G, Chen Y, Tao M, Wu C, Shen X, Yang H. Electrochemical properties of $La_{1-x}Sr_xFeO_3$ (x = 0.2, 0.4) as negative electrode of Ni–MH batteries. Electrochim. Acta 2009;54(15):3910–4.
[7] Wang Q, Deng G, Chen Z, Chen Y, Cheng N. Electrochemical hydrogen property improved in nano-structured perovskite oxide $LaFeO_3$ for Ni/MH battery. J. Appl. Phys 2013;113(5):053305.
[8] Deng G, Chen Y, Tao M, Wu C, Shen X, Yang H, Liu M. Electrochemical properties and hydrogen storage mechanism of perovskite-type oxide $LaFeO_3$ as a negative electrode for Ni/MH batteries. Electrochim. Acta 2010;55(3):1120–4.
[9] Bayart A, Katelnikovas A, Blach JF, Rousseau J, Saitzek S. Synthesis, structural and luminescence properties of $(La_{1-x}Ln_x)_2Ti_2O_7$ (Ln = lanthanides) solid solutions. J. Alloys Compd 2016;683:634–46.
[10] Gao Z, Wu L, Lu C, Gu W, Zhang T, Liu G, Li M. The anisotropic conductivity of ferroelectric $La_2Ti_2O_7$ ceramics. J. Eur. Ceram. Soc 2017;37(1):137–43.
[11] Rittman DR, Turner KM, Park S, Fuentes AF, Yan J, Ewing RC, Mao W. High-pressure behavior of $A_2B_2O_7$ pyrochlore (A = Eu, Dy; B = Ti, Zr). J. Appl. Phys 2017;121(4):045902.

Please cite this article in press as: Henao J, et al. Lanthanum titanate nanometric powder potentially for rechargeable Ni-batteries: Synthesis and electrochemical hydrogen storage. J Mater Res Technol. 2018. https://doi.org/10.1016/j.jmrt.2018.05.019

[12] Saitzek S, Shao Z, Bayart A, Roussel P, Desfeux R. Perovskites and Related Mixed Oxides: Concepts and Applications, 1. Germany: Wiley-VCH; 2015.
[13] Rida K, Peña M, Sastre E, Martínez-Arias A. Effect of calcination temperature on structural properties and catalytic activity in oxidation reactions of $LaNiO_3$ perovskite prepared by Pechini method. J. Rare Earths 2012;30(3):210–6.
[14] Ding XZ, Qi ZZ, He YZ. Effect of hydrolysis water on the preparation of nano-crystalline titania powders via a sol-gel process. J. Mater. Sci. Lett 1995;14(1):21–2.
[15] Uno M, Kosuga A, Okui M, Horisaka K, Yamanaka S. Photoelectrochemical study of lanthanide titanium oxides, $Ln_2Ti_2O_7$ (Ln = La, Sm, and Gd). J. Alloys Compd 2005;400(1):270–5.
[16] Segal D. Chemical synthesis of ceramic materials. J. Mater. Chem 1997;7(8):1297–305.
[17] Li C, Zuo H, Zhang M, Han J. Fabrication of transparent YAG ceramics by traditional solid-state-reaction method. Trans. Nonferrous Met. Soc. China 2007;17(1):148–53.
[18] Mohamedi M, Sato T, Itoh T, Umeda M, Uchida J. Cyclic voltammetry and AC impedance of $MmNi_{3.55}Co_{0.75}Mn_{0.4}Al_{0.3}$ alloy single-particle electrode for rechargeable Ni/MH battery. J. Electrochem. Soc 2002;149(8):A983–7.
[19] Feng F, Northwood DO. Self-discharge characteristics of a metal hydride electrode for Ni–MH rechargeable batteries. Int. J. Hydrogen Energy 2005;30(12):1367–70.
[20] Kaabi A, Tliha M, Dhahri A, Khaldi C, Lamloumi J. Study of electrochemical performances of perovskite-type oxide $LaGaO_3$ for application as a novel anode material for Ni–MH secondary batteries. Ceram. Int 2016;42(10):11682–6.
[21] Liu C, Neale ZG, Cao G. Understanding electrochemical potentials of cathode materials in rechargeable batteries. Mater. Today 2016;19(2):109–23.
[22] Liao B, Lei YQ, Chen LX, Lu GL, Pan HG, Wang QD. A study on the structure and electrochemical properties of $La_2Mg(Ni_{0.95}M_{0.05})_9$ (M = Co, Mn, Fe, Al, Cu, Sn) hydrogen storage electrode alloys. J. Alloys Compd 2004;376(1):186–95.
[23] Cui N, Luan B, Zhao HJ, Liu HK, Dou SX. Effects of yttrium additions on the electrode performance of magnesium-based hydrogen storage alloys. J. Alloys Compd 1996;233(1–2):236–40.
[24] Yuan Y, Dong Z, Li Y, Zhang L, Zhao Y, Wang B, Han S. Electrochemical properties of $LaFeO_3$–rGO composite. Prog. Nat. Sci 2017;27(1):88–92.
[25] Nishina T, Ura H, Uchida I. Determination of chemical diffusion coefficients in metal hydride particles with a microelectrode technique. J. Electrochem. Soc 1997;144(4):1273–7.
[26] Zheng G, Popov BN, White RE. Electrochemical determination of the diffusion coefficient of hydrogen through an $LaNi_{4.25}Al_{0.75}$ electrode in alkaline aqueous solution. J. Electrochem. Soc 1995;142(8):2695–8.
[27] Wang Q, Chen Z, Chen Y, Cheng N, Hui Q. Hydrogen storage in perovskite-type oxides ABO_3 for Ni/MH battery applications: a density functional investigation. Ind. Eng. Chem. Res 2011;51(37):11821–7.
[28] Li M, Yang CC, Wang CC, Wen Z, Zhu YF, Zhao M, Jiang Q. Design of hydrogen storage alloys/nanoporous metals hybrid electrodes for nickel–metal hydride batteries. Sci. Rep 2016;6:27601.

Please cite this article in press as: Henao J, et al. Lanthanum titanate nanometric powder potentially for rechargeable Ni-batteries: Synthesis and electrochemical hydrogen storage. J Mater Res Technol. 2018. https://doi.org/10.1016/j.jmrt.2018.05.019